Neutron-induced transmutation effects in W and W-alloys in a fusion environment

M.R. Gilbert and J.-Ch. Sublet

EURATOM/CCFE Fusion Association, Culham Science Centre, Abingdon, OX14 3DB, UK

E-mail: mark.gilbert@ccfe.ac.uk

Abstract

W and W-alloys are among the primary candidate materials for plasma-facing components in the design of fusion reactors, particularly in high-heat-flux regions such as the divertor. Under neutron irradiation W undergoes transmutation to its near-neighbours in the periodic table. Additionally He and H are particles emitted from certain neutron-induced reactions, and this is particularly significant in fusion research since the presence of helium in a material can cause both swelling and a strong increase in brittleness. This paper presents the results of inventory burn-up calculations on pure W and gives quantitative estimates for He production rates in both a fusion-reactor environment and under conditions expected in the ITER experimental device. Transmutation reactions in possible alloying elements (Re, Ta, Ti and V), which could be used to reduce the brittleness of pure W, are also considered. Additionally, for comparison, the transmutation of other fusion-relevant materials, including Fe and SiC, are presented.

(Some figures in this article are in colour only in the electronic version)

1. Introduction

In the design of fusion power plants and fusion experimental devices, such as ITER, tungsten (W) is being considered for various plasma-facing components because of its desirable structural properties: high melting point, high thermal conductivity and high resistance to sputtering and erosion [1, 2]. As a result, W is a primary candidate material for the divertor armour. These qualities also make W a desirable material for use in other parts of the first wall [3]. However, whereas the divertor armour need only have a lifetime of around two full-power years to make fusion commercially viable [4, 5], the first wall components must be typically able to withstand a fusion environment for at least five years [3, 4]. At these longer times, the irradiation-induced embrittlement of W, which shows significant brittleness to begin with, may become a very serious issue, and both modellers and experimentalists are seeking ways to make W more resilient to these effects.

The ductility of W can be improved through the addition of certain alloying elements such as Re, Tc, Ru, Os, Ti and Co [6]. Some of these, such as Co, would be undesirable in fusion applications because of their unfavourable activation characteristics under neutron irradiation (in the fusion environment Co becomes around 100 times more activated than Fe [7]), but others have shown promising results. Re, in particular, has been found to reduce the ductile–brittle transition temperature (DBTT) of W, and significantly improve

ductility [6], and both mechanical resistance and hardness at room temperature [8], even in concentrations exceeding 25% [8, 9]. However, Nemoto *et al* [1] have questioned the suitability of such a material because of its tendency to form sigma-phase precipitates under neutron irradiation, which leads to hardening and embrittlement. At the same time, it has been observed that alloying W with Re can dramatically reduce its swelling under high dose irradiation [10]. Ta, which is widely used to alloy low activation ferritic–martensitic steels [11] in order to reduce their DBTT [12], has also been proposed as a possible alloying element for W, along with V and Ti, with particular research emphasis on structural applications in a fusion reactor (for example, see [13]).

Of further significance in the design of W and W-alloy materials for fusion applications is their burn-up under neutron irradiation. Specifically, the absorption of a neutron by a nucleus, and the subsequent emission of other particles (whose precise nature depends on the energy of the incident neutron), changes the atomic number and/or the mass number of the original nuclide. This process, known as transmutation or burn-up, may result in the accumulation of residual products that could be either detrimental or beneficial to the mechanical and engineering properties of the original material. Additionally, some of the possible neutron-absorption reactions can lead to the production of charged particles and gases. These light-nuclei elements diffuse through the bulk material and cluster in existing cracks or

in grain boundaries, leading to an increased brittleness (or hardening) of the material.

There have been previous studies on the transmutation of W, such as the irradiation experiments of Noda *et al* [14], and the inventory calculations of Forty *et al* [15] (using an early version of the FISPACT inventory code—see below), but there is an urgent need to update and clarify the situation in W and its possible alloys. This work more fully evaluates the W-transmutation calculations introduced in [2] by Cottrell, and considers the transmutation characteristics of various alloying elements—both as isolated pure samples and as part of a possible W-alloy. Additionally, He and H are important transmutation products and are given special attention in the work.

For comparison, the burn-up of other fusion-relevant materials, namely Fe, Fe-Cr, SiC, Cu and Be, are also presented.

2. Calculation method

To characterize the transmutation properties of W and W-alloys in a fusion-like environment calculations have been carried out using the inventory code developed and maintained by the United Kingdom Atomic Energy Authority over the last 20 years. This inventory code, known as FISPACT, was developed to perform calculations of the activation induced by neutrons (and deuterons and protons [16]) bombarding materials in fusion devices. As well as calculating the activity in a material after a particular irradiation, or indeed after a period of post-irradiation cooling, it also keeps track of the nuclide inventory with time.

Together with external libraries of reaction cross sections and decay data on all relevant nuclides, FISPACT forms the European Activation SYstem (EASY) [16]. FISPACT uses the libraries to calculate the inventory of nuclides (atoms) produced during the irradiation of a starting material composition with a specified flux and spectrum of neutrons (or deuterons or protons). The reference libraries are collectively known as the European Activation File (EAF), and for the present work EAF-2003 [17] has been used.

More recently, EAF-2010 [18], which is currently being compiled and validated, has been used to repeat the calculations presented below for EAF-2003. The results are in good agreement and there are no significant changes to the production levels of He or H. However, we restrict our attention to the results generated using EAF-2003, because the libraries associated with this release have been properly validated.

To perform calculations on a given set of starting materials, FISPACT requires a neutron spectrum for the incident particles. This spectrum (effectively a probability distribution for neutron energies), which is supplied by the user, is collapsed with the cross section data (in units of barns [$=10^{-24}$ cm^2]) to produce a group-averaged library for all reactions available in EAF. This library is then used for all subsequent calculations for the given spectrum. In this work, we have considered spectra calculated for two different fusion environments. The first spectrum, following previous work to describe the activation characteristics of all naturally occurring elements [7, 19], is a relevant first wall (of a fusion device) spectrum from the recent Power Plant Conceptual Study

(PPCS) [3, 4]. Specifically, a neutron spectrum calculated for the first wall of model B, which has a total flux of 1.04×10^{15} n cm^{-2} s^{-1} [20]. The energy profile of the source neutrons used in the calculations (performed with MCNP, see [21] for more details) followed a Gaussian distribution with a peak at the correct 14.1 MeV for the deuterium–tritium (DT) fusion reaction [20]. In line with the expected lifetime of first wall components, the total irradiation time was five years in all calculations with this spectrum.

The second spectrum (or rather spectra-pair) used is one calculated for the first wall of the ITER experimental device, which is currently under construction in France. ITER is expected to operate for two years with a deuterium-only plasma (DD), followed by 12 years of DT operation [22]. Correctly modelling the transmutation response in this case requires two separate spectra, one for each plasma-source type. For the DT plasma, the source-neutron energy profile used in an MCNP calculation on the ITER geometry was the same Gaussian distribution as used for the PPCS-B calculations, while for the deuterium-only reactions of the DD plasma the peak energy was shifted to 2.45 MeV, which is the energy of the neutrons produced during the reaction of two deuterium nuclei [23]. However, the deuterium–deuterium reaction has a second branch of almost equal probability, which has tritium as one of the reaction products. It is not known for certain how much of this tritium will remain confined long-enough to react with deuterium, but current estimates put the fraction anywhere from 20% to 100% [24]. Given that the 2.45 MeV neutrons are produced at a rate of 3.5×10^{18} n s^{-1}, this could mean that an equivalent number of 14.1 MeV neutrons are also produced. In this study we have taken a conservative approach and assumed that confinement is 100%, and so the resulting spectrum for the DD plasma, corresponding to a source producing 7×10^{18} n s^{-1}, is an equal superposition of the DT and deuterium-only spectra. It is also assumed that ITER will be operated at a constant level of approximately 3300 400 s pulses per year throughout the 14 years. This level is planned during the DT phase, but is probably too optimistic for the DD phase. Even with this conservative approach it is important to realize that the calculated transmutation response during the two-year DD phase is insignificant compared with the 12 years of DT operation with its 1.77×10^{20} n s^{-1} neutron source during a typical 500 MW plasma burn (for example see figure 6, where there is a sudden increase in the rate of transmutation after two years). The total first wall fluxes for these ITER spectra during each pulse are 2.38×10^{14} n cm^{-2} s^{-1} and 8.97×10^{12} n cm^{-2} s^{-1}, for the DT and DD phases, respectively.

Figure 1 shows the three neutron spectra, plotted as neutron flux per lethargy interval against energy in eV. A lethargy interval is the standard measure for spectra of this type, and is equal to the natural logarithm of the current energy group's upper bound divided by its lower bound. For the PPCS-B and ITER-DT spectra, there is a clear peak at 14.1 MeV associated with the source-neutron energy, and corresponding to these neutrons hitting the wall directly from the plasma, while for the ITER-DD spectrum this peak is lowered and joined by a peak at the 2.45 MeV deuterium–deuterium neutron energy. In all three cases, there is also a broad spectrum of reduced energy neutrons at a lower level of flux. These neutrons are produced by the scattering and slowing down of neutrons within the particular plant structure.
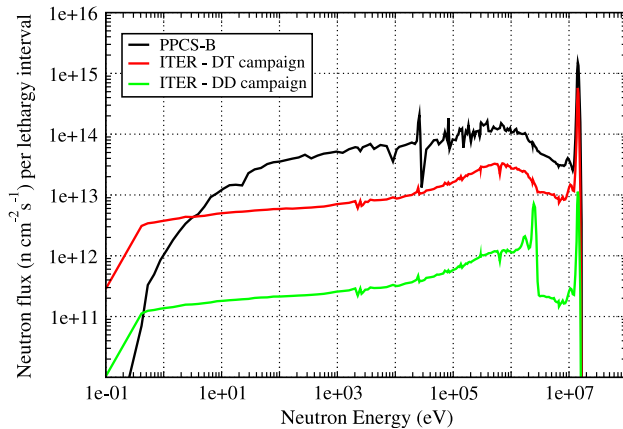
Figure 1. Neutron spectra for the first wall of the model B conceptual power-plant design [20], as well as the spectra for the two neutron-producing campaigns of ITER.

Table 1. Isotropic abundance of the naturally occurring composition of elements considered in this study. Taken from [25].

Element	Atomic number	Atomic mass (u)	Isotopes (% abundance)
Be	4	9.012	^{9}Be (100.0)
C	6	12.011	^{12}C(98.89), ^{13}C (1.11) ^{14}C (Trace)
Si	14	28.086	^{28}Si (92.23), ^{29}Si (4.683) ^{30}Si (3.087)
Ti	22	47.867	^{46}Ti (8.25), ^{47}Ti (7.44) ^{48}Ti (73.72), ^{49}Ti (5.41) ^{50}Ti (5.18)
V	23	50.942	^{50}V (0.25), ^{51}V (99.75)
Cr	24	51.996	^{50}Cr (4.345), ^{52}Cr (83.789) ^{53}Cr (9.501), ^{54}Cr (2.365)
Fe	26	55.845	^{54}Fe (5.845), ^{56}Fe (91.754) ^{57}Fe (2.119), ^{58}Fe (0.282)
Cu	29	63.546	^{63}Cu (69.17), ^{65}Cu (30.83)
Ta	73	180.948	^{180m}Ta (0.012) ^{181}Ta (99.988)
W	74	183.840	^{180}W (0.12), ^{182}W (26.50) ^{183}W (14.31), ^{184}W (30.64) ^{186}W (28.43)
Re	75	186.207	^{185}Re (37.4), ^{187}Re (62.6)

The spectra described above have been used in FISPACT calculations to predict the transmutation of 1 kg pure samples of the elements or 1 kg samples of specific W-alloy compositions. For the PPCS-B power-plant spectrum the material irradiation was in the form of a continuous full-power operation for the full five years. For the ITER first wall irradiation, rather than modelling each pulse individually, a continuous irradiation was performed with the fluxes adjusted to produce the correct overall neutron fluence. Thus, following the 'safety operating scenario' [22], for the two-year DD phase, a continuous flux of 3.75×10^{11} n cm^{-2} s^{-1} was used to model the 3300 pulses, each 400 s long, per year. Similarly, during the first 10 years of DT operation, a single continuous flux of 9.79×10^{12} n cm^{-2} s^{-1} was used. The final two years of the DT campaign were modelled more explicitly, including an 8-month major shutdown period followed by almost 16 months of full operation (with the usual pulse frequency, modelled by a flux of 1.97×10^{13} n cm^{-2} s^{-1}), and a final series of 3 pulses in which the power is increased from the nominal 500 MW to 700 MW [22] (total flux increases to 3.33×10^{14} n cm^{-2} s^{-1}).

Note that in all cases the starting composition of a particular element followed the naturally occurring abundances of its nuclide isotopes. Table 1 shows the naturally occurring nuclide make-up of the elements considered in this study. For example, pure W is made up of five different isotopes, one of which, ^{180}W, forms only a very small fraction (0.12%), while the other four are more abundant. ^{184}W is the most common, making up 30.64% of naturally occurring W.

2.1. Self-shielding effect

One further point concerning the calculations is the issue of correctly accounting for resonance self-shielding. From their initial 14 MeV energy, neutrons will slow down to the thermal energy range. In doing so they will encounter both the unresolved and then the resolved resonance energy regions. In these regions, particularly in heavy elements such as W and its neighbours in the periodic table, the cross sections tend to have a great deal of structure and have sudden and significant variations [26], as can be seen in figures 2 and 3. Of particular importance in these graphs are the giant resonances of the ^{182}W, ^{183}W and ^{186}W isotopes in the 1–100 eV energy range

(^{184}W has none in this region). Monte Carlo neutron-transport codes, such as MCNP, use a continuous point-wise cross section data representation, which allows these resonances to be accurately modelled and accounted for. In the absence of a material with resonances, the neutron flux calculated by a transport code as a function of energy has a generally smooth profile, but in materials containing heavy elements such as W or uranium (U) there are sharp depressions in the neutron flux at the resonance edges where the absorption cross section is massive and dominant. In a well-moderated neutron environment (e.g. in the presence of cooling water), these dips can produce a substantially reduced overall absorption reaction rate. This is the effect known as self-shielding.

Whilst using point-wise cross section data reveals the self-shielding effect, it is not so easy to model its impact on transmutation rates in an inventory code, such as FISPACT, where both the cross sections and neutron spectra are described in a group-wise structure with cross sections computed for infinitely dilute materials. Resonances, which correspond to sharp fluctuations, will instead be represented in a group-wise structure as a 'pillar' of increased cross section in the appropriate energy group. Figure 2(b) illustrates this coarsening. In a coarse neutron energy-group structure this can lead to a significant overestimation, which is compounded by the fact that the self-shielding depressions are not represented. If the spectra shown in figure 1 were to be those actually experienced in resonant elements such as W, then the group absorption reaction rates derived from them would indeed lead to such an overestimation.

Rather than attempt to calculate accurate first wall spectra for each material considered in this study, we have taken an approach whereby the level of overestimation (in the inventory calculation) of the reaction rate for certain absorption reactions is determined by comparison with appropriate MCNP simulations. These 'correction factors' are then used to
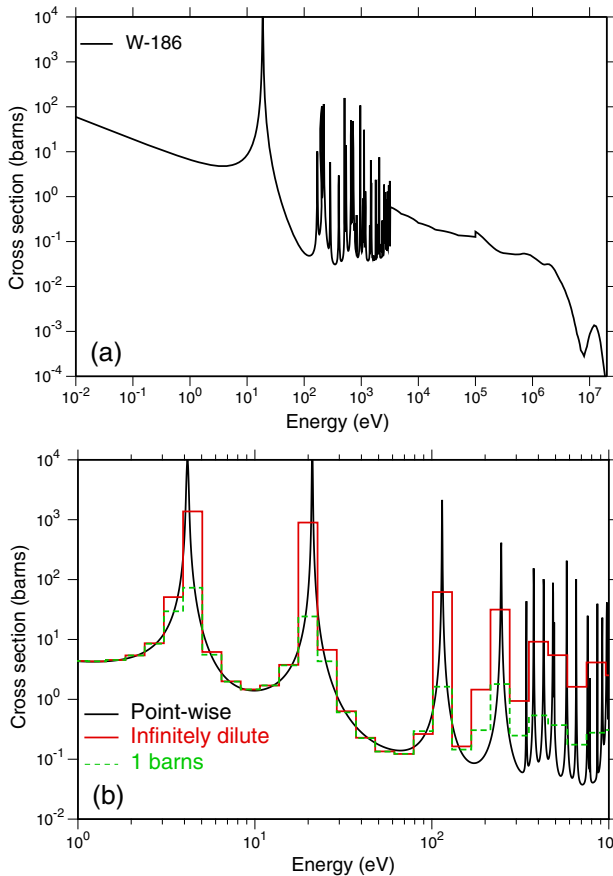
Figure 2. (*a*) The point-wise (n, γ) absorption cross section for ^{186}W, and (*b*) an overlay plot showing how infinitely dilute and 1 barns cross sections in the Vitamin-J energy-group structure compare with the full point-wise cross section data of the ^{182}W (n, γ) reaction in the important resonance regions. From ENDF/B-VII at 293.6 K.

Figure 3. Close-up of the resonance energy regions for the main isotopes of W, with ^{182}W and ^{184}W in (*a*) and ^{183}W and ^{186}W in (*b*). From ENDF/B-VII at 293.6 K.

correct the group-averaged response for these same reactions in the main calculations, performed using the fusion-relevant spectra discussed previously. This means that the subsequent transmutation calculations for different materials are both comparable because of the same neutron spectra are used throughout, but also realistic because self-shielding effects have been accounted for.

We performed a series of MCNP neutron-transport calculations on simple spherical geometries surrounding a fusion-neutron point-source to obtain the reaction rates, total neutron fluxes, and hence group-averaged cross sections (reaction rate divided by total flux) of the (n, γ) reactions for the main naturally occurring isotopes of W, Ta and Re. The 175-group Vitamin-J neutron spectra provided by these calculations were then used in FISPACT to determine the same group-averaged responses. Note that the depressions in these spectra were removed to more accurately reflect the difference between the FISPACT collapsing process, and the fully realized self-shielding effect in MCNP. If the depressions had been left-in, then they would have partially mitigated the effect, leading to an underestimation of the problem.

In each MCNP simulation the material composition was a mixture of metal (one of W, Ta or Re with natural abundances) together with sufficient water to produce the level of neutron-energy moderation required to realize a noticeable
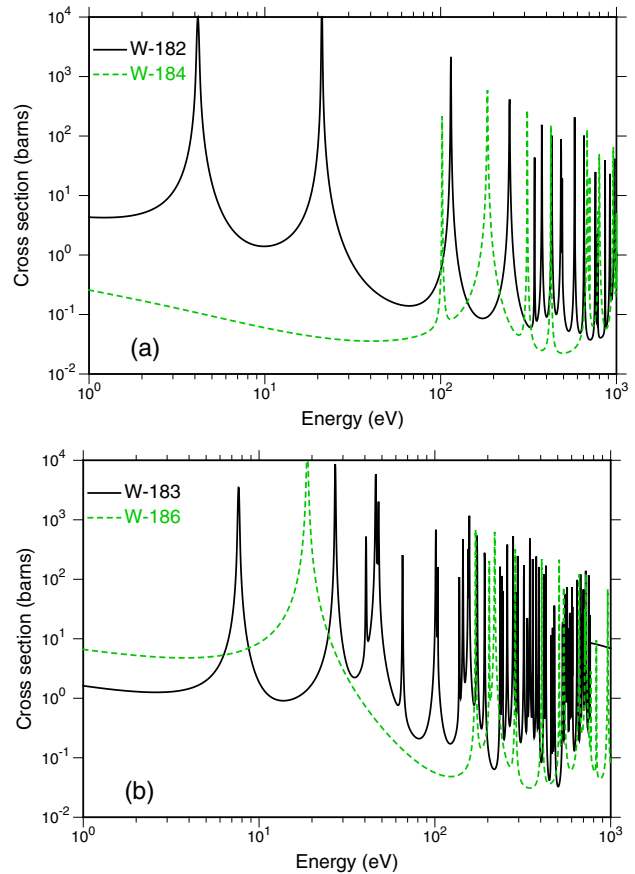
self-shielding effect, and, in particular, to reflect the moderated spectra calculated for representative fusion devices shown in figure 1. The actual percentage of water varied according to the metal being considered. Interestingly, it was observed that pure W acts as a good neutron moderator and so only 20% water (by weight) was added to produce a well-moderated spectrum. Re and Ta, however, are less efficient as neutron moderators, and so a 50–50 metal-water mixture was used in these cases. Note that in actual plasma-facing components the levels of water present could be somewhat different from those considered here because of the cooling requirements, which are at least as important as those of neutron shielding.

The flux and reaction-rate tallies were measured in volumes surrounding the source as a function of depth into the particular metal–water composition, ranging from the first 1 mm layer at the surface exposed to the neutron source up to a 1 cm layer at a depth of 0.3 m. Even though the material thicknesses considered here are greater than might be expected for layers of W (or W-alloy) in the plasma-facing components of a fusion reactor, it was important to perform a scoping study of the self-shielding phenomenon. However, it turned out that while the group-averaged responses showed significant variation as a function of depth, the overestimation factor did not vary a great deal, which gives confidence to the resulting correction factors that are the average overestimation factor across all depths. Note that a proper $S(\alpha, \beta)$ bound thermalization treatment was included

for H$_2$O (with a free gas model applied to all other nuclides). Without any thermal scattering (stationary), neutrons continue to slow down in energy and never form a thermal spectrum, while in contrast, using free atom scattering (proper bound or free gas model), the spectrum diverges from this continuous slowing down and eventually forms a Maxwellian-like thermal spectrum [27]. In the event, the $S(\alpha, \beta)$ treatment was not found to have any noticeable effect on reaction rates because, in the absorption reactions considered here, the giant resonances generally occurred at slightly higher neutron energies than those influenced by it, which are below 4 eV [26].

Figure 4 shows an example 175-group spectrum obtained from MCNP, together with the adjusted spectrum used in FISPACT to obtain the group-averaged response for comparison. It shows the spectrum obtained at the 7–8 cm depth in an 80–20 tungsten–water mix exposed to 14.1 MeV neutrons. Note that in this case the fluxes are those output by MCNP and have units of neutrons per cm^2 per source neutron (n_s). The spectra are also presented as step graphs, where the flux per lethargy spans the entire width of the corresponding energy group. Two depressions are clearly visible in the raw spectrum from MCNP, corresponding to the giant resonances of ^{182}W at 4.2, and the combined effect of the resonances at 21.1 eV, 27.1 eV and 18.8 eV, of ^{182}W, ^{183}W and ^{186}W, respectively (see figure 3). There are also two smaller depressions corresponding to other resonances of ^{183}W at 7.7 and 46.1 eV. In this particular case FISPACT, using the collapsed infinitely dilute data, overestimates the local reaction rates for ^{182}W, ^{183}W, ^{184}W and ^{186}W by factors of 6.92, 3.64, 2.35 and 12.13, respectively, compared with MCNP.

Table 2 gives the self-shielding factors resulting from the calculations described above. ^{186}W, with its single giant resonance at 18.8 eV, has the largest correction factor, while ^{182}W has a somewhat lower factor. From figure 2 we see that ^{183}W has giant resonances that are much closer together than in comparison with those of ^{186}W or ^{182}W. In a coarse group-energy format this results in a reduced correction factor of 3.73 for ^{183}W. ^{185}Re, ^{181}Ta also have a cluster of resonances in their absorption cross sections. ^{184}W and ^{187}Re have the lowest correction factor because their resonances are at higher energy and of lesser magnitude.

For all the subsequent results presented in this study, the factors calculated here were used to correct the group-averaged cross sections for the relevant (n, γ) absorption reactions before the FISPACT inventory calculations were performed. Calculations where the self-shielding correction was not included have also been performed to illustrate the magnitude of the effect. However, the self-shielding corrections, as discussed here, only influence the transmutation results if either W, Re or Ta are present in the material (at any stage during the irradiation).

We note that these correction factors, while leading to a vast improvement compared with calculations where self-shielding is ignored, only go part of the way in providing an exact picture of the transmutation response of materials with large resonances in their capture cross sections. Specifically, we have only taken into account isotopic resonance self-shielding. In practice, the overlapping of resonances between different elements, for example in a material containing both W and Re, would lead to similar combined effects. Further studies of these aspects are being undertaken.
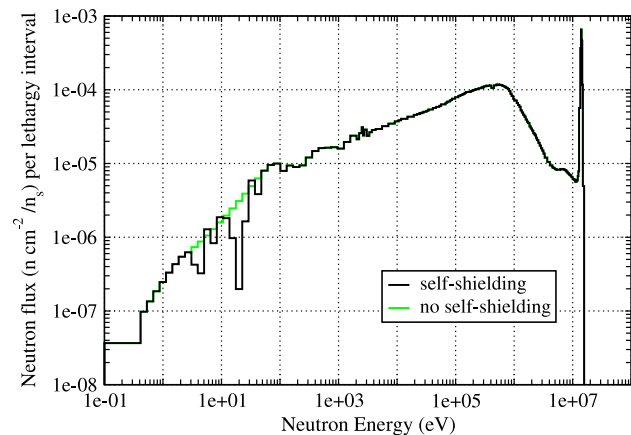

Figure 4. Neutron spectrum in a 1 cm layer at 7–8 cm depth into W (with 20% water by weight) irradiated by fusion neutrons. The raw spectrum (black) shows the local depressions that result from self-shielding, while the second spectrum has these removed.

Table 2. Self-shielding factors (SSFs).

Nuclide	SSF
^{182}W	7.00
^{183}W	3.73
^{184}W	2.36
^{186}W	12.26
^{185}Re	2.80
^{187}Re	2.25
^{181}Ta	3.21

3. Results

Figure 5 shows how W transmutes during the 5-year power-plant first wall irradiation, while figure 6 shows the results from the simulated 14-year ITER campaign. The graphs show the relative concentrations, in atomic parts per million (appm), on a logarithmic scale of the elements present in the sample during the course of the irradiation. Note that in the graphs, and in the other transmutation graphs presented later, elements present in the starting composition (in this case just W) are underlined in the legend. In addition, only those elements whose concentration exceeds one appm after five years of irradiation are included (H and He excepted). In reality, FISPACT calculates the production of many minor elements, and while there may be billions (or more) of atoms of such elements present in the system, the actual appm concentration is extremely small—a fact made clear by realizing that in a one kilogram sample of pure W, there are of the order of 10^{24} atoms of W.

Atomic parts per million (appm) are used for the concentrations shown in the graphs (and all others) because this is the measure that is the most useful for material modellers, where they are interested in how many atoms of the base element should be replaced by atoms of an alloying element. Also, the alternative representation, weight parts per million (wppm), is misleading as far as the production of He and H is concerned because in wppm units these light elements will always appear rare in the transmutation of a much heavier element such as W. Table 3 summarizes the power-plant transmutation results for W and the other materials considered
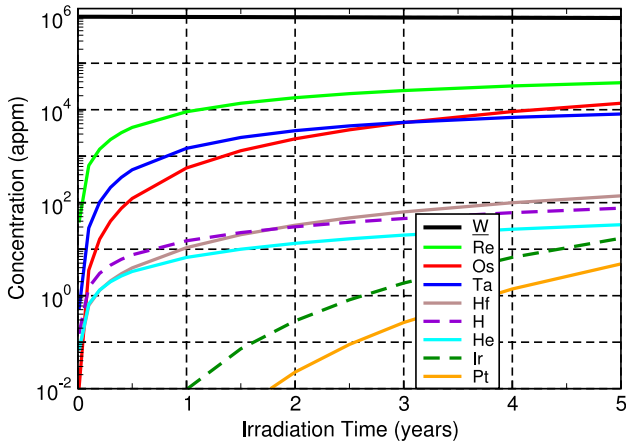
Figure 5. Transmutation of W during a 5-year irradiation under first wall fusion power-plant conditions. Elements appear in the legend in decreasing order of concentration after five years.
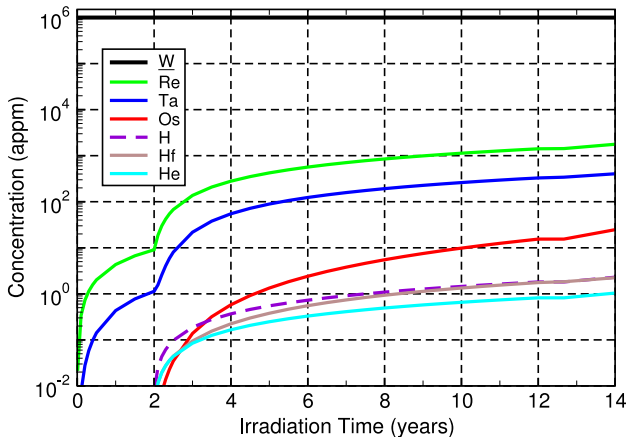

Figure 6. Transmutation of W during a 14-year neutron-irradiation campaign for ITER. Elements appear in the legend in decreasing order of concentration after five years.

in this study, and table 4 does likewise for the transmutation results for the first wall of ITER, with appm concentrations given to three significant figures. Along with He and H, transmutation products are shown in the tables if they reach concentrations greater than 10 000 appm (1 atomic (atm)%) after five years under power-plant conditions, or 1000 appm (0.1 at%) after the 14-year ITER simulation.

In comparing the two graphs shown in figures 5 and 6, it is clear that the level of transmutation predicted for ITER conditions is lower by orders of magnitude. This general trend is repeated in all of the materials considered in this study. It is therefore likely that changes produced by transmutation reactions will not be a cause for concern at any stage during the lifetime of the ITER experiment. Consequently, while the results for ITER are summarized in table 4, they are not discussed further in the subsequent sections.

At the start, before any irradiation takes place, W makes up 100% of the sample, and so in figure 5 the curve for W starts from 1×10^6 appm. As the irradiation proceeds, the amount of W begins to decrease, as some of the W atoms are transformed, through neutron capture reactions and radioactive decays, into other elements. However, the reduction is only slight, with W atoms still at concentrations of 9.4×10^5 appm (94 at%)

after the 5-year irradiation. This is why the (black) curve for W is almost indistinguishable from the grid-line representing 1×10^6 appm. As we shall see later, in other elements, such as Ta (see figure 7), the rate of burn-up (transmutation) can be much greater, causing the reduction in the starting material to become noticeable on the logarithmic scale of the graphs.

The primary transmutation products for W are Re, Os and Ta. Under power-plant conditions, the calculations reveal that Re reaches a concentration of 3.8×10^4 appm (3.8 at%) after five years, with Os at a slightly lower level of 1.38×10^4 appm (1.4 at%) and Ta lower still at only 8.09×10^3 appm (0.81 at%). These could be considered as significant levels, but are much lower than would have been obtained if we had not taken into account the effect of self-shielding. Using the same conditions as before, but without the correction factors in table 2, FISPACT calculations reveal that after five years the concentration of Re would have been 1.18×10^5 appm (11.8 at%), while the Os concentration would be even higher at 1.27×10^5 appm (12.7 at%). This significant discrepancy demonstrates the importance of considering self-shielding when considering materials such as W. As was noted by Cottrell [2], a W–Os–Re alloy composition suggested by the results with no inclusion of self-shielding is very close to the σ-field of the equilibrium ternary phase diagram after the 5-year irradiation. This would imply the possible formation of σ-phase precipitates, which would be both denser and more brittle that the original bcc (α-phase) structure. Subsequent high tensile stresses produced by both shrinkage and in-service mechanical working could lead to cracking and crumbling of these precipitates, causing a weakening of the material as a whole. However, in the modified transmutation results, the resulting concentrations of Re and Os are much lower, suggesting that the formation of precipitates is less likely. We note also that in a later study by Cottrell *et al* [12], where self-shielding effects were considered for ^{186}W alone, they found similar levels of reduced transmutation to those shown in figure 5 for the power-plant irradiation conditions.

Figure 5 also shows that there are several minor transmutation products produced at levels greater than 1 appm after five years. Apart from He and H, we also find significant contributions from Hf, Ir and Pt, although these are only present at concentrations of 141 appm, 17 appm and 5 appm, respectively, after five years. These other metals are only present at low levels because of the relatively long reaction pathways required to produce them from the original W isotopes. For example, a sequence of four (n, γ) capture reactions and β^- decays are needed to transform ^{186}W into ^{190}Pt, which is the shortest possible pathway from a stable isotope of W to a stable (almost) isotope of Pt ((n, γ) and β^- are generally the commonest reactions that increase the neutron and/or proton number).

Curves for H and He are also shown in figure 5. Hydrogen is typically produced during (n, p) reactions, whilst helium originates mainly from (n, α) (neutron capture followed by α-particle (^{4}He ion) emission). The calculations show that H is produced at a level of around 80 appm, while He is produced at a slower rate, with a concentration of around 30 appm at the end of the five-year irradiation. The significance of these results will depend on how W behaves as gas is produced within it, but, as we shall see later, the concentrations are

Table 3. Power-plant transmutation response summary for W and its possible alloying elements, together with several other fusion-relevant materials. For each material, the evolution of a transmutation product is shown if after the 5-year, first wall irradiation it has reached a concentration greater than 1×10^4 appm (1 at%). He and H production results are also given. Concentrations displayed in both appm and at%, with 10 000 appm equivalent to 1 at%.

Starting composition (at%)	Transmutation products	Concentration of product in appm (in brackets, at%) after irradiating for		
		1 year	3 years	5 years
W (100)	W	9.89×10^5 (98.9)	9.63×10^5 (96.3)	9.40×10^5 (94.0)
	Re	9.06×10^3 (0.91)	2.59×10^4 (2.59)	3.80×10^4 (3.80)
	Os	5.58×10^2 (0.06)	5.28×10^3 (0.53)	1.38×10^4 (1.38)
	He	6.65×10^0 (<0.01)	2.00×10^1 (<0.01)	3.36×10^1 (<0.01)
	H	1.51×10^1 (<0.01)	4.56×10^1 (<0.01)	7.63×10^1 (<0.01)
Ta (100)	Ta	9.32×10^5 (93.2)	7.56×10^5 (75.6)	6.15×10^5 (61.5)
	W	6.37×10^4 (6.37)	2.32×10^5 (23.2)	3.67×10^5 (36.7)
	Hf	4.37×10^3 (0.44)	1.15×10^4 (1.15)	1.67×10^4 (1.67)
	He	2.88×10^0 (<0.01)	1.03×10^1 (<0.01)	2.00×10^1 (<0.01)
	H	1.64×10^1 (<0.01)	5.07×10^1 (<0.01)	8.68×10^1 (<0.01)
Re (100)	Re	8.73×10^5 (87.3)	6.65×10^5 (66.5)	5.08×10^5 (50.8)
	Os	1.22×10^5 (12.2)	3.20×10^5 (32.0)	4.69×10^5 (46.9)
	W	5.67×10^3 (0.57)	1.50×10^4 (1.50)	2.15×10^4 (2.15)
	He	3.58×10^0 (<0.01)	1.14×10^1 (<0.01)	1.98×10^1 (<0.01)
	H	1.89×10^1 (<0.01)	5.81×10^1 (<0.01)	9.82×10^1 (<0.01)
Ti (100)	Ti	9.99×10^5 (99.9)	9.97×10^5 (99.7)	9.95×10^5 (99.5)
	He	1.83×10^2 (0.02)	5.48×10^2 (0.05)	9.13×10^2 (0.09)
	H	5.95×10^2 (0.06)	1.79×10^3 (0.18)	2.98×10^3 (0.30)
V (100)	V	9.98×10^5 (99.8)	9.93×10^5 (99.3)	9.88×10^5 (98.8)
	He	7.26×10^1 (<0.01)	2.18×10^2 (0.02)	3.63×10^2 (0.04)
	H	5.16×10^2 (0.05)	1.55×10^3 (0.16)	2.58×10^3 (0.26)
Fe (100)	Fe	9.98×10^5 (99.8)	9.93×10^5 (99.3)	9.87×10^5 (98.7)
	He	2.19×10^2 (0.02)	6.56×10^2 (0.07)	1.09×10^3 (0.11)
	H	1.01×10^3 (0.10)	3.01×10^3 (0.30)	5.01×10^3 (0.50)
Fe–9% Cr alloy	Fe	9.08×10^5 (90.8)	9.03×10^5 (90.3)	8.98×10^5 (89.8)
Fe (91)	Cr	9.00×10^4 (9.00)	9.00×10^4 (9.00)	9.01×10^4 (9.00)
Cr (9)	He	2.14×10^2 (0.02)	6.40×10^2 (0.06)	1.06×10^3 (0.11)
	H	9.90×10^2 (0.10)	2.96×10^3 (0.30)	4.92×10^3 (0.49)
SiC	Si	4.98×10^5 (49.8)	4.94×10^5 (49.4)	4.90×10^5 (49.0)
Si (50)	C	4.98×10^5 (49.8)	4.94×10^5 (49.4)	4.90×10^5 (49.0)
C (50)	He	2.28×10^3 (0.23)	6.79×10^3 (0.68)	1.13×10^4 (1.13)
	H	8.60×10^2 (0.09)	2.56×10^3 (0.26)	4.25×10^3 (0.43)
C (100)	C	9.96×10^5 (99.6)	9.88×10^5 (98.8)	9.80×10^5 (98.0)
	He	3.50×10^3 (0.35)	1.04×10^4 (1.04)	1.73×10^4 (1.73)
	H	2.96×10^0 (<0.01)	8.98×10^0 (<0.01)	1.53×10^1 (<0.01)
Cu (100)	Cu	9.89×10^5 (98.9)	9.68×10^5 (96.8)	9.48×10^5 (94.8)
	Ni	6.05×10^3 (0.61)	1.80×10^4 (1.80)	2.97×10^4 (2.97)
	Zn	2.71×10^3 (0.27)	8.01×10^3 (0.80)	1.31×10^4 (1.31)
	He	2.14×10^2 (0.02)	6.40×10^2 (0.06)	1.06×10^3 (0.11)
	H	1.49×10^3 (0.15)	4.43×10^3 (0.44)	7.33×10^3 (0.73)
Be (100)	Be	9.93×10^5 (99.3)	9.79×10^5 (97.9)	9.66×10^5 (96.6)
	He	6.57×10^3 (0.66)	1.96×10^4 (1.96)	3.24×10^4 (3.24)
	H	1.02×10^2 (0.01)	3.79×10^2 (0.04)	7.48×10^2 (0.07)

very low compared with those found in some of the more traditional fusion materials. Note that the gas production levels are largely unaffected by the inclusion/omission of the self-shielding corrections because all of the elements near to W in the periodic table (in the same transition metal row) have very similar gas production rates from transmutation.

3.1. Transmutation of possible alloying elements

As mentioned in the introduction, the extreme brittleness of pure W is a significant concern to those designing and planning future fusion experiments and reactors. One possible solution to this may be found by alloying W with certain other metals. This study considers four possible alloying elements: tantalum (Ta), rhenium (Re), titanium (Ti) and vanadium (V). In all cases the irradiation conditions used in FISPACT were the same as those used above for W.

For Ta, the transmutation evolution under a 5-year power-plant irradiation is shown in figure 7. Comparing this figure with the equivalent one for W in figure 5, it is obvious that Ta undergoes much greater rates of transmutation than W, even when accounting for self-shielding in the capture cross section

Table 4. ITER transmutation response summary for W and its possible alloying elements, together with several other fusion-relevant materials. For each material, the evolution of a transmutation product is shown if after the 14-year ITER campaign it has reached a concentration greater than 1×10^3 appm (0.1 at%). He and H production results are also given. Concentrations displayed in both appm and at%, with 10 000 appm equivalent to 1 at%.

Starting composition (at%)	Transmutation products	Concentration of product in appm (in brackets, at%) after irradiating for		
		2DD years	2DD+6DT years	2DD+12DT years
W (100)	W	1.00×10^6 ($\approx$100)	9.99×10^5 (99.9)	9.98×10^5 (99.8)
	Re	9.07×10^0 (<0.01)	8.49×10^2 (0.08)	1.77×10^3 (0.18)
	He	3.26×10^{-3} (<0.01)	4.92×10^{-1} (<0.01)	1.04×10^0 (<0.01)
	H	7.21×10^{-3} (<0.01)	1.09×10^0 (<0.01)	2.29×10^0 (<0.01)
Ta (100)	Ta	1.00×10^6 ($\approx$100)	9.91×10^5 (99.1)	9.81×10^5 (98.1)
	W	8.91×10^1 (<0.01)	8.74×10^3 (0.87)	1.84×10^4 (1.84)
	He	1.31×10^{-3} (<0.01)	2.01×10^{-1} (<0.01)	4.29×10^{-1} (<0.01)
	H	7.83×10^{-3} (<0.01)	1.18×10^0 (<0.01)	2.49×10^0 (<0.01)
Re (100)	Re	1.00×10^6 ($\approx$100)	98.6×10^5 (98.6)	9.71×10^5 (97.1)
	Os	1.60×10^2 (0.02)	1.33×10^4 (1.33)	2.76×10^4 (2.76)
	W	9.11×10^0 (<0.01)	8.67×10^2 (0.09)	1.79×10^3 (0.18)
	He	1.67×10^{-3} (<0.01)	2.60×10^{-1} (<0.01)	5.60×10^{-1} (<0.01)
	H	9.02×10^{-3} (<0.01)	1.36×10^0 (<0.01)	2.86×10^0 (<0.01)
Ti (100)	Ti	1.00×10^6 ($\approx$100)	1.00×10^6 ($\approx$100)	1.00×10^6 ($\approx$100)
	He	9.08×10^{-2} (<0.01)	1.37×10^1 (<0.01)	2.88×10^1 (<0.01)
	H	3.00×10^{-1} (<0.01)	4.45×10^1 (<0.01)	9.35×10^1 (<0.01)
V (100)	V	1.00×10^6 ($\approx$100)	1.00×10^6 ($\approx$100)	9.99×10^5 (99.9)
	He	3.60×10^{-2} (<0.01)	5.43×10^0 (<0.01)	1.14×10^1 (<0.01)
	H	2.59×10^{-1} (<0.01)	3.90×10^1 (<0.01)	8.21×10^1 (<0.01)
Fe (100)	Fe	1.00×10^6 ($\approx$100)	1.00×10^6 ($\approx$100)	1.00×10^6 ($\approx$100)
	He	1.09×10^{-1} (<0.01)	1.65×10^1 (<0.01)	3.47×10^1 (<0.01)
	H	5.08×10^{-1} (<0.01)	7.53×10^1 (<0.01)	1.58×10^2 (0.02)
Fe–9%Cr alloy	Fe	9.10×10^5 ($\approx$91)	9.10×10^5 ($\approx$91)	9.10×10^5 ($\approx$91)
Fe (91)	Cr	9.00×10^4 ($\approx$9)	9.00×10^4 ($\approx$9)	9.00×10^4 ($\approx$9)
Cr (9)	He	1.07×10^{-1} (<0.01)	1.61×10^1 (<0.01)	3.39×10^1 (<0.01)
	H	4.99×10^{-1} (<0.01)	7.40×10^1 (<0.01)	1.56×10^2 (0.02)
SiC	Si	5.00×10^5 ($\approx$50)	5.00×10^5 ($\approx$50)	5.00×10^5 ($\approx$50)
Si (50)	C	5.00×10^5 ($\approx$50)	5.00×10^5 ($\approx$50)	5.00×10^5 ($\approx$50)
C (50)	He	1.13×10^0 (<0.01)	1.70×10^2 (0.02)	3.59×10^2 (0.04)
	H	4.29×10^{-1} (<0.01)	6.48×10^1 (<0.01)	1.36×10^2 (0.01)
C (100)	C	1.00×10^6 ($\approx$100)	1.00×10^6 ($\approx$100)	9.99×10^5 (99.9)
	He	1.73×10^0 (<0.01)	2.61×10^2 (0.03)	5.49×10^2 (0.05)
	H	9.26×10^{-4} (<0.01)	1.38×10^{-1} (<0.01)	2.90×10^{-1} (<0.01)
Cu (100)	Cu	1.00×10^6 ($\approx$100)	9.99×10^5 (99.9)	9.98×10^5 (99.8)
	He	1.07×10^{-1} (<0.01)	1.61×10^1 (<0.01)	3.40×10^1 (<0.01)
	H	8.05×10^{-1} (<0.01)	1.12×10^2 (0.01)	2.36×10^2 (0.02)
Be (100)	Be	1.00×10^6 (100)	9.99×10^5 (97.9)	9.99×10^5 (99.9)
	He	3.53×10^0 (<0.01)	4.83×10^2 (0.05)	1.02×10^3 (0.10)
	H	4.08×10^{-2} (<0.01)	6.10×10^0 (<0.01)	1.33×10^1 (<0.01)

of its primary stable nuclide (^{181}Ta). At the end of the five years its concentration has fallen from the initial 100% to only 61.6% (6.16×10^5 appm). The main transmutation product is W, which reaches a concentration of 3.67×10^5 appm (36.7 at%), with Hf produced at a lower level, reaching 1.4 at% after five years. We note that without the self-shielding correction, the results would have been very different. In line with previous studies [2, 15], W would have reached a majority concentration of 76%, while Ta would have made up only 23% of the final material after five years. However, the 36.7% W obtained in this work is still a large amount.

If these burn-up levels for Ta are true then alloying W with Ta might provide an interesting alternative to pure W. During irradiation, a W–Ta alloy would become more W, but would

also not produce as much of the other transmutation products such as Re or Os (these are only produced at a low level in the pure Ta calculations). In fact, if the composition was chosen carefully, it is conceivable that the concentration of W could be kept constant under fusion neutron-irradiation, thereby preserving the desirable mechanical properties associated with this metal.

In Re, there are also relatively high levels of burn-up of the starting material. Os reaches a concentration of 4.69×10^5 appm or 46.9% after five years (this would have been 7.6×10^5 appm or 76% if we had not made a self-shielding adjustment), while Re drops to 5.08×10^5 appm (50.8%) over the same period (W makes a minor 2.15% contribution to the overall composition). The likely consequence of the high
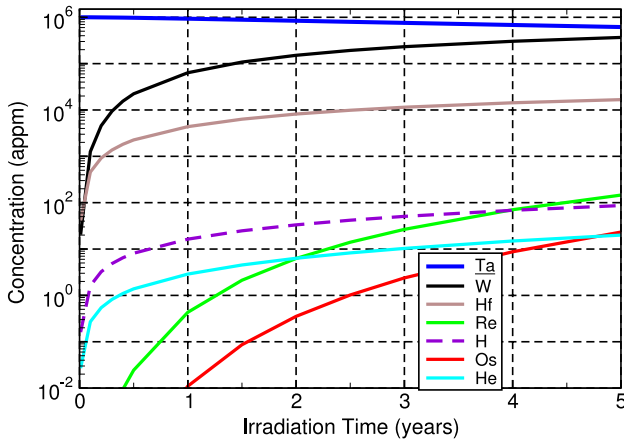
Figure 7. Transmutation of Ta during a 5-year irradiation under first wall fusion power-plant conditions. Elements appear in the legend in decreasing order of concentration after five years.
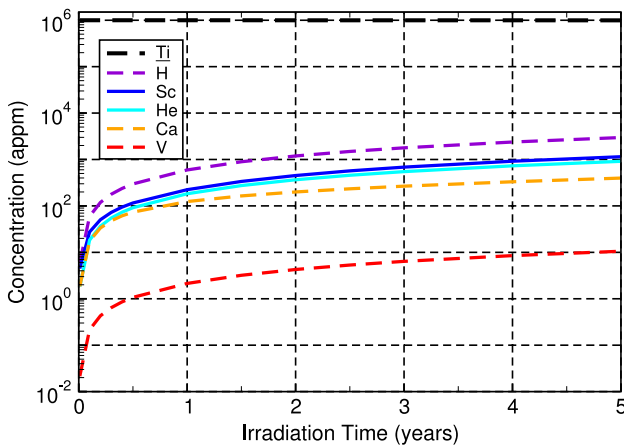

Figure 8. Transmutation of Ti during a 5-year irradiation under first wall fusion power-plant conditions. Elements appear in the legend in decreasing order of concentration after five years.

Table 5. Final material composition summary for W alloyed with several transition metals at a level of 30 at%. For each alloy, the final concentration of a transmutation product is shown if it has reached a level greater than 1×10^4 appm (1 at%) after the 5-year power-plant irradiation. He and H production results are also given. Concentrations displayed in both appm and at%, with 10 000 appm equivalent to 1 at%.

Starting composition (at%)	Transmutation products	Concentration of product in appm (in brackets, at%)
W–30% Ta alloy	W	7.68×10^5 (76.8)
	Ta	1.90×10^5 (19.0)
W (70)	Re	2.67×10^4 (2.67)
Ta (30)	He	2.95×10^1 (<0.01)
	H	7.95×10^1 (<0.01)
W–30% Re alloy	W	6.64×10^5 (66.4)
	Re	1.79×10^5 (17.9)
W (70)	Os	1.50×10^5 (15.0)
Re (30)	He	2.95×10^1 (<0.01)
	H	8.29×10^1 (<0.01)
W–30% Ti alloy	W	6.57×10^5 (65.7)
	Ti	2.99×10^5 (29.9)
W (70)	Re	2.66×10^4 (2.66)
Ti (30)	He	2.98×10^2 (0.03)
	H	9.49×10^2 (0.09)
W-30%V alloy	W	6.57×10^5 (65.7)
	V	2.97×10^5 (29.7)
W (70)	Re	2.66×10^4 (2.66)
V (30)	He	1.33×10^2 (0.01)
	H	8.30×10^2 (0.08)

transmutation rates for Re is that it would be undesirable as an alloying element for W because of the increased chance of σ-phase precipitates as Os is produced.

For Re and Ta the gas production (He and H) rates are broadly similar to those observed in W, with 20 appm He produced in both Re and Ta during the 5-year power-plant scenario (compared with ~30 appm in W), and 98 and 87 appm H for Re and Ta, respectively, under the same conditions.

However, if we now consider the results of the two other possible alloying elements, then the gas production levels are significantly higher. Even though the burn-up of Ti and V is much slower than in any of W, Ta or Re (their respective concentrations remain around 99 or 100 at% after irradiation—see table 3), the levels of He and H production are at least an order of magnitude greater. Figure 8, which shows the transmutation response of pure Ti, demonstrates this low overall transmutation but high gas production (the greatest transmutation product is in fact H, but this only reaches a concentration of 0.3 at% after five years). He achieves a concentration of 913 and 363 appm after a 5-year power-plant irradiation in Ti and V, respectively, while H reaches concentrations of 2978 and 2191 appm. In Ti, Sc is the only

other transmutation product produced in significant amounts, while in V, Cr and Ti both reach thousands of appm after five years.

In summary, for these four elements we observe that, if alloyed to W, neither Re or Ta would cause the levels of He or H to be significantly increased, while Ti and V, however, could cause the levels to increase significantly. The exact level of increase is dependent on the amount of the starting material that is made up of the alloying element (i.e. the alloying per cent), and below we consider, as an illustration, the compositional changes that would take place in a W material that has been alloyed with one of these elements to a level of 30 at%.

3.2. Combined effects in alloys

Above we observed that there maybe some desirable and not-so-desirable transmutation consequences associated with alloying W with one of Ta, Re, Ti or V. As an example of what might be expected in an actual W-alloy, we have calculated the transmutation response for W alloyed with one of these metals to a level of 30 at%. This is probably greater than what would be used in reality (especially for the lighter Ti and V), and so this illustration can be viewed as an upper limit in terms of the effect (on transmutation response) that alloying has in W. Note, however, that Re has been considered experimentally as an alloying element of W in concentrations of up to 26% (either by weight or atoms) [1, 8].

Table 5 shows the final material compositions resulting from additional FISPACT calculations, where the starting material is adjusted to contain 70 at% W and 30 at% of an alloying metal. Relevant calculations were performed for
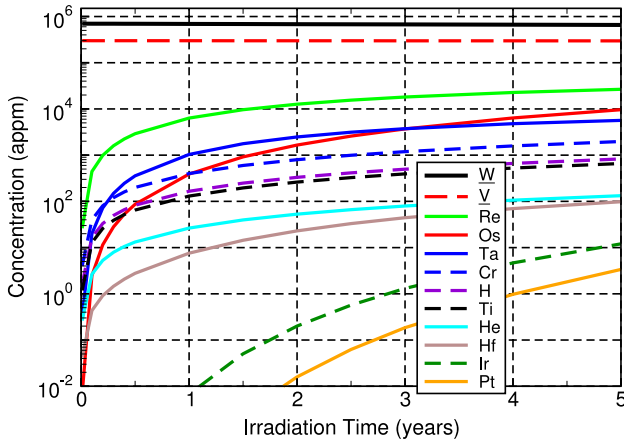
Figure 9. Transmutation of a W–30% V (by atoms) alloy during a 5-year irradiation under first wall fusion power-plant conditions. Elements appear in the legend in decreasing order of concentration after five years.

both the 5-year power-plant and the 14-year ITER scenarios, although only the former are presented in the table (as usual, the burn-up predicted under ITER is of no significance). Since each of the four alloying metals considered have different atomic masses, the actual percentage by weight (required by FISPACT) that each contributes to a 70–30 by atom % alloy varies. Using the atomic masses from table 1 the weight percentages used in this illustrative study are calculated as 30.269%, 29.668%, 10.039% and 10.615% for Re, Ta, Ti and V, respectively, with W making up the rest.

For W–30 at% Ta and W–30 at% Re, the levels of He and H production are relatively similar to the pure W case (see table 3), and are once again around the 30 appm and 80 appm mark, respectively, after the 5-year power-plant irradiation. However, as expected, in the other two alloys considered the levels of He and H production are significantly greater (∼10 times). 298 appm He and 949 appm H are produced during the 5-year power-plant scenario in W–30 at% Ti, while in W–30 at% V He and H reach concentrations of 133 appm and 830 appm, respectively. These findings demonstrate that the level of gas production under neutron-irradiation induced transmutation is an important factor to consider when choosing elements with which to alloy W, which on its own does not produce He or H to any significant levels. Figure 9 shows the evolution of the transmutation products during the 5-year power-plant first wall irradiation of W–30 at% V.

On the other hand, since Ti and V do not undergo the same level of burn-up as Re and Ta, even though gas production is higher, the benefits associated with alloying W using Ti or V, such as reducing brittleness, may be maintained for longer during irradiation than in W alloyed with Re or Ta, whose concentrations in the material will fall noticeably over time.

3.3. Comparison with other fusion materials

For perspective, we also consider the transmutation response of some of the other primary candidate materials for in-vessel components of fusion reactors.

Steels are widely used in both experimental fusion devices and nuclear fission reactors, and will certainly be the main

structural material used in future fusion devices and reactors. Fe is the primary constituent of steels, and in ferritic–martensitic steels (body-centred cubic structure or bcc) makes up more than 80 wt% of the total. Meanwhile, Cr is the main alloying element in reduced-activation ferritic–martensitic (RAFM) because it helps to reduce the radiation-induced swelling of the steel [28], which is a significant problem in the popular austenitic steels (face-centred cubic or fcc) [29, 30]. The exact % of Cr to be added to Fe is still being debated, although Fe–9 at% Cr is perhaps the most widely studied so far. At concentrations significantly above this level, at fusion operating temperatures and irradiation levels, Cr begins to segregate into clusters, causing a loss of ductility and corrosion resistance [31, 32], while below 9% Cr remains in solute and exhibits short-range ordering [31, 33]. The transmutation characteristics of both pure Fe and Fe–9 at% Cr are discussed below.

Alternatively, silicon carbide (SiC) composites are also considered as possible first wall structural materials because of their low activation characteristics under neutron irradiation [34]. They also show good fracture resistance and have excellent high temperature mechanical properties (see, for example, Raffray *et al* [35], Jones *et al* [36], and Riccardi *et al* [37]). A basic SiC compound was considered in this work, which implies a 50–50 mix by atoms of Si and C. In mass terms this corresponds to 70.045% by weight Si and 29.955% by weight C (i.e. Si has a higher atomic mass).

High strength Cu alloys, such as Cu–Cr–Zr, are the primary heat sink materials for structural components in the high-heat-flux regions of fusion devices [38], including the first wall and divertor [4, 39]. Cu has high thermal conductivity, although its high sputtering yield prohibits use as a plasma-facing component [40]. Meanwhile, Be exhibits strong neutron thermalization and multiplication properties, and also has good thermal characteristics [41], which, together with its low effect on the plasma when present as a contaminant [39] (due to low atomic mass), make Be highly desirable as a plasma-facing material and neutron multiplier in fusion-reactor design. Below we consider the transmutation response of pure Cu (for simplicity) and Be under the first wall spectrum.

Figure 10 shows the burn-up response of a 1 kg sample of pure Fe under the 5-year first wall power-plant irradiation conditions. As with Ti and V, which are both in the same row of the periodic table (transmutation trends follow rows, rather than groups), the transmutation of Fe is minor. The most common elements after five years are Mn and H, but these are only produced at concentrations of 5.5×10^3 appm and 5×10^3 appm, respectively, which, in percentage terms, are both around 0.5%. He is produced at concentrations reaching 1100 appm, which is higher than in Ti and V, and more than a factor of 10 greater than in W. This trend in He production under irradiation agrees qualitatively with previous studies. For example, Übeyli and Demir [42] have recently calculated He production in possible structural alloys in a fusion first wall as a function of the thickness of a thorium molten salt liquid shield layer, which has been proposed as a way to avoid frequent replacement of the first wall. They observed the greatest He production, at all liquid layer thicknesses, in ferritic steels (i.e. predominantly Fe), with V-alloys slightly better, and a W–Re alloy the best of all, with an order of magnitude less He produced compared with the other two.
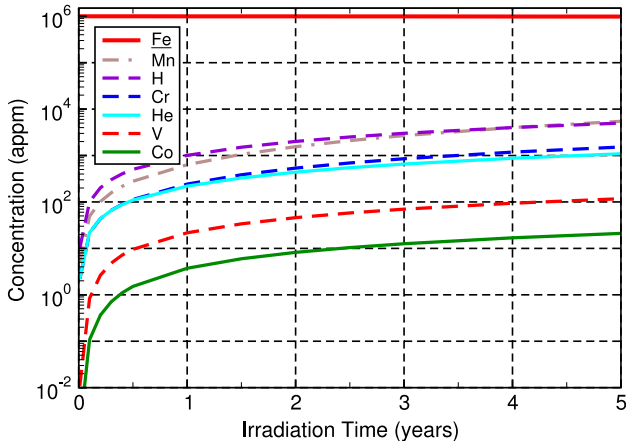
Figure 10. Transmutation of Fe during a 5-year irradiation under first wall fusion power-plant conditions. Elements appear in the legend in decreasing order of concentration after five years.

Adding 9 at% Cr to Fe has very little effect on the transmutation characteristics. From table 3, it is clear that compared with pure Fe (figure 10), the only differences in composition after five years, apart from the presence of 9% Cr, are that Ti now appears as a minor product and the amount of V has increased slightly, but these are present in very small amounts (around 0.01% and 0.1% of the total, respectively). He and H production levels are almost identical to those seen in pure Fe.

In experimental studies of Fe–9% Cr martensite it has been found that bubbles of He can significantly increase brittleness when present at concentrations of around 5×10^3 appm [43, 44], although it is not clear if the same effect would be observed at the lower He concentrations predicted in the present calculations, and there is also H to consider. In any event, it is likely that ferritic/martensitic steels (austenitic steels are known to suffer from He embrittlement at concentrations as low as 10 appm [45]) can withstand slightly higher levels of He (and H) impurity than W and W-alloys because of the (current) difficulties in manufacturing these latter materials. Whereas the melting point of Fe (and hence steels) is around 1500 K, W has a melting point of 3410 K, which makes the production of large quantities of homogeneous metal very difficult, and many of the current processing techniques (such as sintering of W powder or pellets) lead to an irregular and perhaps already weakened microstructure in the final product. Of course, it is also possible that in the future, perhaps in response to an increased demand, better fabrication processes will be developed, and so the W-based components used in future fusion reactors may be no worse (or may be better) than steels for He embrittlement.

In the transmutation of SiC, the production of He is very high, with only Be producing more in this study. After five years of power-plant irradiation, the concentration of He is around 11 000 appm or 1.1% of the total atoms, and even under ITER conditions it is fairly significant, reaching 360 appm after 14 years. These numbers are 10 times higher than in Fe and 100 times greater than in W, and are in good agreement with previous calculations, where He production was estimated to be around 2000 appm per year and around 10000 appm during power-plant component lifetime [46, 47]. H production is

also very high, with 4250 appm produced under power-plant conditions.

While the transmutation of Si does contribute to the production of He, it is from reactions on C (specifically ^{12}C) that most is generated. Indeed, if we consider the transmutation of C alone (see table 3) then we find that the production of He is 50% greater than what it is in SiC. Even more interesting is the fact that H production from C is almost negligible compared with the production from SiC, being three orders of magnitude lower than in SiC. In fact, if the transmutation evolution from pure Si is calculated (not shown in the tables) then the H production is almost exactly twice that found in SiC, confirming that reactions on Si atoms are responsible for almost all of the H produced. Specifically, from Si, H is the main transmutation product (although He, Mg and Al reach concentrations of the same order of magnitude), while in C He is produced at levels ten times greater than the next largest transmutation product (Be), with H languishing in third, another order of magnitude lower. In SiC, after He and H, the remaining transmutation products are all produced in small amounts, with Mg the most significant at around 0.26 at% of the total after the 5-year power-plant irradiation.

The burn-up of Cu is higher than in the other first-row transition metal elements (Ti, V and Fe) discussed so far, and the total reduction of the starting material after the 5-year power-plant irradiation is broadly the same as in W. In the case of Cu, the main transmutation products are Ni (2.97×10^4 appm or 2.97 at% after the power-plant irradiation) and Zn (1.31×10^4 appm or 1.31 at%), which are the immediate neighbours of Cu in the periodic table. These values are in reasonable agreement with the results of Garner *et al* [48] produced using the STARFIRE fusion spectrum, and also the calculations of Butterworth [49] obtained from a conceptual fusion-neutron spectrum, where in both cases they found a few % of Ni and around 1% Zn (either atomic or weight %).

It is well known that Ni, and to a lesser extent Zn, strongly influence the thermal conductivity of Cu, with conductivity falling with increasing concentration of these transmutation products [48–50]. This effect may have a significant impact on design of a fusion device, and so it is worth noting it again here to illustrate the complexities associated with the materials specification for a fusion environment.

The He production rates in Cu are about the same as those calculated for Fe and Ti, while the concentration of H after five years is greater than in any other material considered in this study at 7.33×10^3 appm (0.73 at%) under power-plant conditions, in good agreement with approximately 1 at% calculated by Garner *et al* [48].

Finally, in Be, the calculations reveal that He reaches a concentration of 3.24×10^4 appm after five years of power-plant fluxes, which is three times greater than in SiC which itself produces an order of magnitude more He than Fe, Cu or Ti (the next highest group). Recent experiments by Chakin *et al* [51] found that neutron-irradiations producing He concentrations of the order of 2×10^4 appm (similar to the levels calculated here for the power-plant spectrum) lead to between 2.2% and 4.3% swelling in Be, while Möslang *et al* [52] found that high-temperature annealing after irradiation could produce swelling rates of 17%. Chakin *et al* [51] found that the He-induced swelling was accompanied by an embrittlement

of the material (due to grain-boundary weakening by swelling voids) and hence a reduction in strength. Thus, the production of He via transmutation under neutron irradiation has a direct life-limiting effect on components constructed using Be.

On the other hand, H production rates are quite low in Be, with less than 1000 appm produced during the five-year first wall irradiation, although analysis of the calculation results indicates that in this case the major H isotope produced is ^{3}H (tritium), which is highly radioactive. This contrasts with the H production seen in the other materials considered in this study, where the H production occurs primarily through the (n, p) reaction leading to ^{1}H. Thus in Be, H production is a significant issue even at the relatively low levels found here, but for activation considerations rather than for radiation-induced swelling. Of course, this tritium production pathway could be useful in a fusion reactor as an additional source of fuel, although the transmutation of Li remains the primary candidate in this respect. The only other transmutation product to reach a significant concentration in Be is Li, which is produced at about the same rate as H.

3.4. Isotope tailoring

Another important consideration when investigating the transmutation phenomenon is the relative contribution to certain transmutation products from the different isotopes (of the same element) present in the starting composition. For example, as shown in table 1, naturally occurring W is made up of 5 isotopes, with three of these each contributing around 30% of the total. Under the right circumstances, which may be financially motivated, it may be possible to influence the transmutation response of an element by altering the relative concentrations of its isotopes ('isotope tailoring'), while leaving other physical and mechanical properties unaffected.

Here we investigate how the final composition of the material changes after irradiating pure 1 kg samples of each of the five different naturally occurring isotopes of W. We consider the same 5-year power-plant irradiation as before. The final compositions from the appropriate FISPACT calculations are shown in table 6.

The results from this isotope study demonstrate that for W, the production of Re and Os, which may be undesirable for both the mechanical properties and the activation characteristics, could be mitigated by reducing the relative concentration of ^{186}W in the elemental composition of the W because it is from this isotope that the production of Re and Os is greatest. There is no doubt that there are other isotope tailoring opportunities, leading to improved behaviour of materials under neutron irradiation, and this should be studied thoroughly as a matter of urgency.

4. Conclusions

This paper describes an investigation into the transmutation properties of W and possible W-alloys. Calculations show that W and its near-neighbours in the periodic table do not produce significant amounts of He or H under neutron-irradiation induced transmutation, especially in comparison with other fusion-reactor elements such as Be and Fe.

Table 6. Transmutation response summary for different isotopes of W, showing how the concentration of W, Ta, Hf, Re and Os varies in the final composition (summed over all isotopes) after the 5-year power-plant irradiation. Concentrations displayed in both appm and at%, with 10 000 appm equivalent to 1 at%.

Starting isotope	Transmutation products	Concentration of product in appm (in brackets, at%)
^{180}W	W	5.83×10^5 (58.3)
	Ta	3.91×10^5 (39.1)
	Hf	2.61×10^4 (2.61)
	Re	2.24×10^1 (<0.01)
	Os	2.78×10^0 (<0.01)
^{182}W	W	9.71×10^5 (97.1)
	Ta	2.84×10^4 (2.84)
	Hf	3.59×10^2 (0.04)
	Re	4.74×10^2 (0.05)
	Os	8.35×10^1 (<0.01)
^{183}W	W	99.2×10^5 (99.2)
	Ta	7.03×10^2 (0.07)
	Hf	8.76×10^1 (<0.01)
	Re	5.48×10^3 (0.55)
	Os	1.32×10^3 (0.13)
^{184}W	W	9.56×10^5 (95.6)
	Ta	3.04×10^1 (<0.01)
	Hf	5.03×10^0 (<0.01)
	Re	3.20×10^4 (3.20)
	Os	1.19×10^4 (1.19)
^{186}W	W	8.69×10^5 (86.9)
	Ta	1.64×10^{-1} (<0.01)
	Hf	6.46×10^{-2} (<0.01)
	Re	9.61×10^4 (9.61)
	Os	3.49×10^4 (3.49)

However, Re and Ta, which are proposed as additions to W to improve its brittleness, seem to undergo significant burn-up to Os and W, respectively. While these results need to be confirmed by more detailed studies, which should focus on all self-shielding effects in mixed material compositions and in specific geometries, confirmation of the significance of these effects may raise serious questions about the suitability of either Re or Ta for use in materials exposed to a fusion-reactor environment. A high transmutation rate, particularly to elements such as Os, could have detrimental effects on structural and mechanical properties of materials and the components constructed from them, and any benefit produced by adding either Re or Ta to W might be jeopardized. On the other hand, in the case of Ta, the production of W as the primary transmutation product might in fact be a unexpected benefit, especially if the percentage of Ta in the W-alloy can be chosen so that its production of W balances-out the transmutation of W into Re.

In W-alloys involving Ti and V, the burn-up of the alloying elements is much lower, meaning that there should be very little evolution (under irradiation) of the material properties produced by adding either of these elements. Unfortunately, this is set against a level of gas production in Ti and V that is much greater (10 times) than in Ta, Re or W. Further study is required to determine the safe levels of He and H in W and W-alloys before the use of Ti or V in alloys can be considered or discounted. Calculations have also revealed that He (and H) production during transmutation is greatest in materials containing lighter elements such as Be or SiC, although there

are notable exceptions, with Cu showing the greatest hydrogen production of the materials studied here.

It is apparent that the production of undesirable elements via transmutation could be mitigated by altering the natural isotopic composition of elements. For example, in W it is possible to reduce the production of Re by reducing the amount of ^{186}W present initially because this isotope is the primary source responsible for Re's production. Even though there is less flexibility in the isotopic composition of either Re or Ta (they each only have two long-lived or stable isotopes), it is possible that an appropriate enrichment may improve the transmutation response. Meanwhile, the prospects for Ti and V could be improved by reducing the isotopes that are chiefly responsible for the gas transmutation products.

Acknowledgments

Euratom © 2011.

References

[1] Nemoto Y., Hasegawa A., Satou M. and Abe K. 2000 *J. Nucl. Mater.* **283–287** 1144–7
[2] Cottrell G.A. 2004 *J. Nucl. Mater.* **334** 166–8
[3] Maisonnier D., Cook I., Sardain P., Boccaccini L., De Pace L., Giancarli L., Norajitra P. and Pizzuto A. 2006 *Fusion Eng. Des.* **81** 1123–30
[4] Maisonnier D. *et al* 2005 *Fusion Eng. Des.* **75–79** 1173–9
[5] Ward D.J., Cook I., Lechon Y. and Saez R. 2005 *Fusion Eng. Des.* **75–79** 1221–7
[6] Mutoh Y., Ichikawa K., Nagata K. and Takeuchi M. 1995 *J. Mater. Sci.* **30** 770–5
[7] Gilbert M.R. and Forrest R.A. 2004 Handbook of Activation Data Calculated Using EASY-2003 *Technical Report* UKAEA FUS 509
[8] Falbriard P., Rochette P. and Nicolas G. 1991 *Refract. Met. Hard Mater.* **10** 37–43
[9] Klopp W.D. 1975 *J. Less-Common Met.* **42** 261–78
[10] Smid I., Akiba M., Vieider G. and Plöchl L. 1998 *J. Nucl. Mater.* **258–263** 160–72
[11] Luo J., Tuo F. and Kong X. 2009 *Phys. Rev.* C **79** 057603
[12] Cottrell G.A., Kemp R., Bhadeshia H.K.D.H., Odette G.R. and Yamamoto T. 2007 *J. Nucl. Mater.* **367–370** 603–9
[13] Aguirre M.V., Martín A., Pastor J.Y., Llorca J., Monge M.A. and Pareja R. 2009 *Metall. Mater. Trans.* A **40** 2283–90
[14] Noda T., Fujita M. and Okada M. 1998 *J. Nucl. Mater.* **258–263** 934–9
[15] Forty C.B.A., Butterworth C.J. and Sublet J.-Ch. 1994 *J. Nucl. Mater.* **212–215** 640–3
[16] Forrest R.A. *et al* EASY-2007 documentation http://www.ccfe.ac.uk/EASY.aspx
[17] Forrest R.A. *et al* EASY-2003 documentation http://www.ccfe.ac.uk/EASY_archive.aspx
[18] Sublet J.-Ch., Packer L.W., Kopecky J., Forrest R.A., Koning A.J. and Rochman D.A. 2010 *The European Activation File* EAF-2010 neutron-induced cross section library, CCFE-R(10)05
[19] Gilbert M.R. and Forrest R.A. 2006 *Fusion Eng. Des.* **81** 1511–6
[20] Pampin-Garcia R. and Loughlin M.J. 2002 Neutronic and activation calculations for PPCS plant model B (HCPB) *UKAEA/EURATOM Fusion Association* PPCS/UKAEA/PPCS4D2-2
[21] Brown F.B. *et al* 2002 *Trans. Am. Nucl. Soc.* **87** 273–6
[22] Loughlin M.J. and Taylor N.P. 2009 Recommended Plasma Scenarios for Activation Calculations *ITER Document Series* ITER-D-2V3V8G v 1.1
[23] Iida H., Khripunov V., Petrizzi L. and Federici G. 2004 *Nuclear Analysis Report*, *ITER Document Series* G 73 DDD 2 W 0.2
[24] How J. and Reichle R. 2009 Plant Design Description *ITER Baseline Document* ITER-D-2X6K67 v1.0
[25] Tuli J.K. 2000 *Nuclear Wallet Cards* 6th edn (Upton, NY: National Nuclear Data Center, Brookhaven National Laboratory)
[26] Sublet J.-Ch. and Sawan M.E. 1999 *Fusion Eng. Des.* **45** 65–73
[27] Cullen D.E., Blomquist R.N., Greene M., Lent E., MacFarlane R., McKinley S., Plechaty E.F. and Sublet J.-Ch 2006 *How Accurately Can We Calculate Neutrons Slowing Down In Water? LLNL Report* no UCRL-TR-220605, US DOE
[28] Garner F.A., Toloczko M.B. and Spencer B.H. 2000 *J. Nucl. Mater.* **276** 123–42
[29] Little E.A. and Stow D.A. 1979 *J. Nucl. Mater.* **87** 25–39
[30] Gelles D.S. 1994 *J. Nucl. Mater.* **212–215** 714–9
[31] Kuwano H. and Hamaguchi Y. 1988 *J. Nucl. Mater.* **155-157** 1071–4
[32] Klueh R.L. and Nelson A.T. 2007 *J. Nucl. Mater.* **371** 37–52
[33] Mirebeau I., Hennion M. and Parette G. 1984 *Phys. Rev. Lett.* **53** 687–690
[34] Dyomina E., Fenici P., Kolotov V. and Zucchetti M. 1998 *J. Nucl. Mater.* **258–263** 1784–90
[35] Raffray A. *et al* 2001 *Fusion Eng. Des.* **55** 55–95
[36] Jones R., Snead L., Kohyama A. and Fenici P. 1998 *Fusion Eng. Des.* **41** 15–24
[37] Riccardi B., Giancarli L., Hasegawa A., Katoh Y., Kohyama A., Jones R. and Snead L. 2004 *J. Nucl. Mater.* **329–333** 56–65
[38] Ishino S., Kurui A., Ichikawa S., Inaba T. and Hasegawa T. 2000 *J. Nucl. Mater.* **283–287** 215–9
[39] 2001 *ITER Technical Basis* Document G A0 FDR 1 01-07-13 R1.0
[40] Krauss A.R., Gruen D.M., Lam N.Q. and Dewald A.B. 1984 *J. Nucl. Mater.* **128–129** 570–6
[41] Leenaers A., Verpoucke G., Pellettieri A., Sannen L. and Van den Berghe S. 2007 *J. Nucl. Mater.* **372** 256–62
[42] Übeyli M. and Demir T. 2008 *Mater. Des.* **29** 852–9
[43] Jung P., Henry J., Chen J. and Brachet J.-C. 2003 *J. Nucl. Mater.* **318** 241–8
[44] Henry J., Mathon M.-H. and Jung P. 2003 *J. Nucl. Mater.* **318** 249–59
[45] van der Schaaf B., Ehrlich K., Fenici P., Tavassoli A.A. and Victoria M. 2000 *Fusion Eng. Des.* **48** 499–508
[46] Hasegawa A., Oliver B., Nogami S., Abe K. and Jones R. 2000 *J. Nucl. Mater.* **283–287** 811–5
[47] Snead L., Jones R., Kohyama A. and Fenici P. 1996 *J. Nucl. Mater.* **233–237** 26–36
[48] Garner F.A., Heinisch H.L., Simons R.L. and Mann F.M. 1990 *Radiat. Eff. Defects Solids* **113** 229–55
[49] Butterworth G.J. 1985 *J. Nucl. Mater.* **135** 160–72
[50] Garner F.A. 1990 *J. Nucl. Mater.* **174** 229–39
[51] Chakin V.P., Posevin A.O. and Kupriyanov I.B. 2007 *J. Nucl. Mater.* **367–370** 1377–81
[52] Möslang A., Pieritz R.A., Boller E. and Ferrero C. 2009 *J. Nucl. Mater.* **386–388** 1052–5